Formation of hydrogen atom in 2s state in proton–sodium inelastic scattering

Sabbah A. Elkilany[a)b)†]

[a)] Department of Mathematics, Faculty of Science, Ad Dammam University, Kingdom of Saudi Arabia
[b)] Department of Mathematics, Faculty of Science, Kafrelsheikh University, Kafrelsheikh, Egypt

(Received 24 June 2014; revised manuscript received 15 August 2014; published online 30 January 2015)

The inelastic collision of protons with sodium atoms are treated for the first time within the framework of the coupled-static and frozen core approximations. The method is used for calculating partial and total cross-sections with the assumption that only two channels (elastic and hydrogen formation in 2s state) are open. In each case, the calculations are carried out for seven values of the total angular momentum $\ell(0 \leq \ell \leq 6)$. The target is described using the Clementi Roetti wave functions within the framework of the one valence electron model. We use Lipmann–Swinger equation to solve the derived equations of the problem, then apply an iterative numerical method to obtain the code of computer to calculate iterative partial cross-sections. This can be done through calculating the reactance matrix at different values of considered energies to obtain the transition matrix that gives partial and total cross sections. The present results for total hydrogen (2s state) formation cross sections are in agreement with results of other available ones in wide range of incident energy.

Keywords: proton–sodium inelastic scattering, hydrogen formation

PACS: 34.80.Dp, 34.80.Gs, 34.80.Ht **DOI:** 10.1088/1674-1056/24/3/033402

1. Introduction

The appearance of intermediate states in atomic and nuclear reactions is considered as the most interesting physical phenomenon since the development of quantum theory. The development of femtosecond lasers has tremendously enhanced the experimental identification of these states in chemical and physical reactions. Theoretical investigation on positron–atom or proton–atom scattering has been carried out by many authors. Most theoretical treatments of positron–atom or proton–atom scattering are based on calculations of differential, partial, and total cross sections as functions of incident energy using different approximations. Abdel-Raouf[1] investigated the collision of positrons by lithium and sodium atoms using the coupled static approximation. Elkilany[2–5] used the variational static approximation or iterative Green's function partial wave expansion method to obtain partial and total cross sections of elastic scattering of positron or electron by inert gas atoms. Surdutovitch *et al.*[6] reported measurements of Ps formation cross sections for positron collision by lithium and sodium atoms. Jun *et al.*[7] discussed positronium formation cross sections for positron collision by potassium at low energies using an optical-model method. Roy and Ho[8] calculated the P-partial wave resonance in e^+–Li scattering below the Ps threshold using the stabilization method. Gilmore *et al.*[9] obtained results for electron– or positron–positronium scattering in low energies using a coupled pseudo-state approximation. Ratnavelu and Ng[10] used the coupled-channel optical method to study positron collision by lithium atom. Abdel-Raouf and Elkilany[11] applied the iterative Green's function partial wave expansion method to calculate partial and total cross sections of the collision of positron by helium, neon, argon, and krypton atoms. Abdel-Raouf and Elkilany[12] discussed the appearance of intermediate states (resonant states) in positron–lithium collision. Elkilany[13] computed the partial and total cross sections of excited positronium formation in the scattering of positrons by positronium using the coupled static approximation. Jun *et al.*[14] calculated the Ps formation cross section in positron collision by lithium atom using the coupled channel optical method. Fang *et al.*[15] used a coupled-channel optical method to calculate positron collision with lithium atom. Banyard and Shirtcliffe[16] used the continuum-distorted wave method to calculate cross sections for protons scattered from atomic lithium. Ferrante *et al.*[17] calculated total cross sections for hydrogen formation in protons scattering with alkali atoms using the OBK approximation. Daniele *et al.*[18] calculated total cross-sections for high-energy proton scattering by alkali atom. Ferrante and Fiordilino[19] investigated high-energy proton collision with alkali atom using the Eikonal approximation. Fritsch and Lin[20] discussed the hydrogen formation in proton scattering by lithium atoms using a modified two-center atomic orbital expansion. Choudhury and Sural[21] calculated the hydrogen formation in the collision of proton with alkali-metal atoms using the wave formulation of impulse approximation. Tiwiri[22] reported the differential and total cross sections in the hydrogen formation in the collision of proton by lithium and sodium atoms using the coulomb projected Born approximation. Elkilany and Abdel-Raouf[23] investigated the

†Corresponding author. E-mail: sabbelkilany@yahoo.com

© 2015 Chinese Physical Society and IOP Publishing Ltd

effect of polarization potentials on antiproton scattered by positronium using coupled static approximation. Elkilany[24] used the coupled static approximation and Green's function iterative method to calculate partial and total cross sections of anti-hydrogen formation in antiproton positronium collision.

For the first time, we investigate the inelastic scattering of protons by sodium atoms as a two-channel problem in which the elastic and hydrogen (2s state), H(2s), formation channels are open using the coupled-static approximation within the framework of the frozen-core picture of Na atom. The considered method has been applied successfully in the inelastic scattering of proton by lithium atom by Elkilany.[25]

2. Theoretical formalism

The two-channel scattering problems under investigation can be sketched by

$$\mathrm{p}+\mathrm{Na}\{3\mathrm{s}\} = \begin{bmatrix} \mathrm{p}+\mathrm{Na}\{3\mathrm{s}\}, & \text{elastic channel,} \\ \mathrm{H}\{2\mathrm{s}\}+\mathrm{Na}^{+}, & \mathrm{H(2s)\ formation\ channel.} \end{bmatrix} \quad (1)$$

The one valence electron model of an alkali target (Na) is described (in Rydberg units) by[1]

$$H_{\mathrm{Na(3s)}} = -\frac{1}{2\mu_{\mathrm{m}}}\nabla_r^2 - \frac{2}{r} + V_{\mathrm{c}}(r), \quad (2)$$

where r is the position vector of the valence electron with respect to the origin of the scattering system, in which the nucleus of the target is infinitely heavy. $V_{\mathrm{c}}(r)$ is a screened potential defined by

$$V_{\mathrm{c}}(r) = V_{\mathrm{cCoul}}(r) + V_{\mathrm{cex}}(r), \quad (3)$$

where $V_{\mathrm{cCoul}}(r)$ and $V_{\mathrm{cex}}(r)$ are the Coulomb and exchange parts of the core potential.

Following Clementi and Roetti,[26] the wave function of the i-th electron in the orbital j of the target is expanded by

$$\Phi_j(r_i) = \sum_{p=1}^{m_j} c_{jp}\chi_{jp}(r_i), \quad (4)$$

where $\left|\chi_{jp}(r_i)\right\rangle$ is a Slater-type wave function given by

$$\chi_{jp}(r_i) = A_{jp} r_i^{k_{jp}} \mathrm{e}^{-\alpha_{jp} r_i} \mathrm{Y}_{jp}(\vartheta_i, \varphi_i). \quad (5)$$

The k_{jp} are integers or zero, A_{jp} are normalization factors determined by

$$A_{jp} = [(2\alpha_{jp})^{2k_{jp}+1}/(2k_{jp})!]^{1/2}, \quad (6)$$

and the spherical harmonics Y_{jp} are normalized by $\left\langle \mathrm{Y}_{jp}(\vartheta_i, \varphi_i) | \mathrm{Y}_{jp}(\vartheta_i, \varphi_i) \right\rangle = 1$. The constants c_{jp} and α_{jp} are adjusted within the framework of the Hatree–Fock–Roothaan approach. Substituting Eq. (5) into Eq. (4) and introducing the notation $\bar{c}_{jp} = c_{jp}A_{jp}$, we obtain

$$\Phi_j(r_i) = \sum_{p=1}^{m_j} \bar{c}_{jp} r_i^{k_{jp}} \mathrm{e}^{-\alpha_{jp} r_i} \mathrm{Y}_{jp}(\vartheta_i, \varphi_i), \quad (7)$$

where m_j is the number of basis functions characteristic to each orbital. Usually, all the orbitals of the same type have the same m_j.

The Coulomb part of the core potential is defined by

$$V_{\mathrm{cCoul}}(r) = \sum_{j=1}^{M}{}' N_j \left\langle \Phi_j(r_i) \right| \frac{2}{|\bar{r} - \bar{r}_i|} - \frac{2}{r} \left| \Phi_j(r_i) \right\rangle, \quad (8)$$

where M is the number of orbitals, and N_j is the number of electrons occupying the orbital j. The prime on the sum sign means that the term $-2/r$ is repeated for each j. The exchange part of the core potential is defined by

$$V_{\mathrm{cex}}(r) = -\sum_{j=1}^{M} \left\langle \Phi_{\mathrm{Na(3s)}}(r_i) \right| \frac{2}{|\bar{r} - \bar{r}_i|} \left| \Phi_j(r_i) \right\rangle, \quad (9)$$

where the subscript Na(3s) is employed for distinguishing the wave function for the valence electron of the target atom.

According to Eq. (2), the binding energy of the valence electron of the target is determined by

$$E_{\mathrm{Na(3s)}} = \left\langle \Phi_{\mathrm{Na(3s)}}(r) \right| H_{\mathrm{Na(3s)}} \left| \Phi_{\mathrm{Na(3s)}}(r) \right\rangle. \quad (10)$$

The total Hamiltonian of the first channel, elastic channel, has the following form (in Rydberg units and frozen core approximation):

$$H = H^{(1)} = H_{\mathrm{T}} - \frac{1}{2\mu_{\mathrm{M}}}\nabla_x^2 + V_{\mathrm{int}}^{(1)}, \quad (11)$$

where μ_{M} is the reduced mass of the first channel. In Fig. 1, $\bar{x}$ and $\bar{r}$ are the position vectors of the projectile proton and the valence electron of the target with respect to the center of mass of target, $\bar{\rho}$ is the position vector of the projectile proton with respect to the valence electron of the target , $\bar{\sigma}$ is the position vector of the center of mass of H(2s) from target, M_{T} is the mass of the nucleus of target, and $V_{\mathrm{int}}^{(1)}$ denotes the interaction between the incident proton and the target atom, i.e.,

$$V_{\mathrm{int}}^{(1)} = \frac{2}{x} - \frac{2}{|\bar{x} - \bar{r}|} + V_{\mathrm{cCoul}}(x), \quad (12)$$

where

$$V_{\mathrm{cCoul}}(x) = -V_{\mathrm{cCoul}}(r)\,|_{r=x}\,, \quad (13)$$

and the corresponding total energy in the first channel is determined by

$$E = E^{(1)} = E_{\mathrm{Na(3s)}} + \frac{1}{2\mu_{\mathrm{M}}} k_1^2. \quad (14)$$

The second term on the right is the kinetic energy of incident proton relative to the target nucleus.

The total Hamiltonian of the second channel, H(2s) formation, is expressed (in Rydberg units and frozen core approximation) as

$$H = H^{(2)} = H_{\mathrm{H(2s)}} - \frac{1}{2\mu_{\mathrm{M}'}}\nabla_\sigma^2 + V_{\mathrm{int}}^{(2)}, \quad (15)$$

where $\mu_{M'}$ is the reduced mass of the second channel, $V_{\rm int}^{(2)}$ represents the interaction between the particles of H(2s) and the rest of the target atom, i.e.,

$$V_{\rm int}^{(2)} = \frac{2}{x} - \frac{2}{r} + V_{\rm cCoul}(x) + V_{\rm cCoul}(r) + V_{\rm cex}(r), \quad (16)$$

and the total energy of the second channel is determined by

$$E = E^{(2)} = E_{\rm H(2s)} + \frac{1}{2\mu_{M'}} k_2^2. \quad (17)$$

The second term on the right is the kinetic energy of center of mass of H(2s) with respect to the nucleus of the target. This is related to the energy of the incident proton by

$$\frac{k_2^2}{2\mu_{M'}} = \left(E_{\rm Na(3s)} + \frac{1}{2\mu_{\rm M}} k_1^2 - E_{\rm H(2s)} \right), \quad (18)$$

where $E_{\rm H(2s)} = -0.25$ Ry is the first excited 2s-state energy of H(2s) and $k_2^2/2\mu_{M'} > 0$ means that H(2s) channel is open, otherwise it is closed. Thus, H(2s) formation is only possible if $k_1^2 > 2\mu_{\rm M}(E_{\rm H(2s)} - E_{\rm Na(3s)})$.

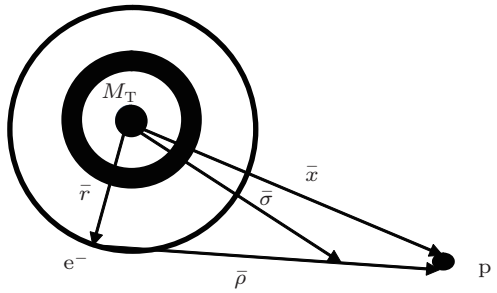


Fig. 1. Configuration space of p–Na scattering.

The coupled static approximation states that the solution of the two-channel scattering problem under consideration is subjected to the following conditions:[25]

$$\langle \Phi_{\rm Na(3s)} | H - E | \Psi \rangle = 0, \quad (19)$$

$$\langle \Phi_{\rm H(2s)} | H - E | \Psi \rangle = 0, \quad (20)$$

where $|\Psi\rangle$ is the total wave function describing each scattering process, i.e.,

$$|\Psi\rangle = \left| \Phi_{\rm Na(3s)}(r) \right\rangle |\psi_1(x)\rangle + \left| \Phi_{\rm H(2s)}(\rho) \right\rangle |\psi_2(\sigma)\rangle, \quad (21)$$

where

$$\Phi_{\rm H(2s)} = \frac{1}{\sqrt{32\pi}} (2-\rho) \exp(-\rho/2) \quad (22)$$

is the ground-state wave function of H(2s), $\psi_1(x)$ is the wave function describing scattered protons, and $\psi_2(x)$ is the scattering wave function of the second channel. Substituting Eqs. (14) and (21) into Eq. (19), we obtain

$$\frac{1}{2\mu_{\rm M}} \left(\nabla_x^2 + k_1^2 \right) |\psi_1\rangle = U_{\rm st}^{(1)}(x) |\psi_1\rangle + \langle \Phi_{\rm Na(3s)} \left| H^{(2)} - E^{(2)} \right| \Phi_{\rm H(2s)} \psi_2 \rangle. \quad (23)$$

Substituting Eqs. (17) and (21) into Eq. (20), we obtain

$$\frac{1}{2\mu_{M'}} \left(\nabla_\sigma^2 + k_2^2 \right) |\psi_2\rangle = U_{\rm st}^{(2)}(\sigma) |\psi_2\rangle + \langle \Phi_{\rm H(2s)} \left| H^{(1)} - E^{(1)} \right| \Phi_{\rm Na(3s)} \psi_1 \rangle, \quad (24)$$

where Schrödinger's equations of the target and H(2s) are employed. The potentials $U_{\rm st}^{(1)}(x)$ and $U_{\rm st}^{(2)}(\sigma)$ are defined by

$$U_{\rm st}^{(1)}(x) = \langle \Phi_{\rm Na(3s)}(r) | V_{\rm int}^{(1)} | \Phi_{\rm Na(3s)}(r) \rangle, \quad (25)$$

$$U_{\rm st}^{(2)}(\sigma) = \langle \Phi_{\rm H(2s)}(\rho) | V_{\rm int}^{(2)} | \Phi_{\rm H(2s)}(\rho) \rangle. \quad (26)$$

Using the partial wave expansions of the scattering wave functions $|\psi_1\rangle$ and $|\psi_2\rangle$ in Eqs. (23) and (24), solutions are given (formally) by the Lippmann–Schwinger equation (see appendix)

$$|\xi\rangle = |\xi_0\rangle + G_0 |\zeta\rangle, \quad (27)$$

where G_0 is the Green operator $(\varepsilon - H_0)^{-1}$ and $|\xi_0\rangle$ is the solution of the homogeneous equation

$$(\varepsilon - {\rm H}_0) |\xi_0\rangle = |0\rangle. \quad (28)$$

The partial wave expansions of Green operators corresponding to operators in the two differential equations enable us to write their solutions in integral form that can be solved by iterative numerical technique. Then we obtain the reactance matrix $\boldsymbol{R}^\nu$ which is related to the transition matrix $\boldsymbol{T}^\nu$

$$\boldsymbol{T}^\upsilon = \boldsymbol{R}^\upsilon \left({\rm I} - \tilde{\rm i} \boldsymbol{R} \right)^{-1}, \quad (29)$$

where ν is the order of iteration, $\boldsymbol{I}$ is a 2×2 unit matrix, and $\tilde{\rm i} = \sqrt{-1}$. Partial cross sections obtained in an iterative way are determined (in πa_0^2 units) by

$$\sigma_{ij}^{\ell,\nu} = \frac{4(2\ell+1)}{k_1^2} |T_{ij}^\nu|^2, \quad i = 1,2. \quad (30)$$

Finally, the total cross sections (in πa_0^2 units) are expressed (in the ν-th iteration) by

$$\sigma_{ij}^\nu = \sum_{\ell=0}^{\infty} \sigma_{ij}^{(\ell,\nu)}, \quad i,j = 1,2, \quad \nu > 0. \quad (31)$$

3. Results and discussion

We begin with testing the variation of static potentials of two channels, $U_{\rm st}^{(1)}(x)$ and $U_{\rm st}^{(2)}(\sigma)$, with increase of x and σ, respectively. Values of x and σ have been chosen such that $x = \sigma = 1/16, 2/16, 3/16, \ldots, 512/16$, where $h = 1/16$ is the mesh size (or Simpson's step) employed to calculate integrals appearing in integral equations using Simpson's rule. Calculation of cross sections of proton–sodium (p–Na) scattering has been proceeded by investigating the variation of the elements

of R^{υ} with the increase of integration range (IR) and the number of iterations. We set h to be 1/16 and use 512 mesh points (i.e., IR = $32a_0$). It is found that excellent convergence can be obtained with $\upsilon = 50$. This demonstrates the stability of our iterative method. Final calculations have been carried out for seven partial waves corresponding to $0 \le \ell \le 6$ at values of k_1^2 representing the kinetic energy region ($10 \le k_1^2 \le 1000$ keV).

Table 1 shows the partial and total elastic cross sections for all incident values of energy between 10 and 1000 keV. We can conclude the following points: (i) the main contributions to the total elastic cross sections, σ_{11}'s, are due to the S and P partial cross sections; (ii) the total elastic cross sections, σ_{11}'s, decrease steadily with k_1^2; (iii) the seven partial waves employed are quite satisfactory to calculate the total elastic cross sections σ_{11}'s to a higher degree of accuracy within the framework of the coupled-static approximation.

In Table 2 we present the partial and total H(2s) formation cross sections, σ_{12}'s, at all considered energies. The values indicate that the results shown in Table 1 have been repeated for the values of partial and total H(2s) formation cross sections, σ_{12}'s. The most interesting results are accumulated in Table 3, where we find a comparison between total H(2s) formation cross sections (in πa_0^2) determined by different authors using different approaches. In column 2, we find the present total H(2s) formation cross sections. Column 3 involves the values of H(2s) formation cross sections obtained by Choudhury and Sural[21] using the wave formulation of impulse approximation. The next column contains the values of total H(2s) formation cross sections of Tiwari[22] in protons scattering with alkali atoms using the coulomb projected Born approximation. In Fig. 2 we also show the present results together with those of Choudhury and Sural[21] and Tiwari[22] in the energy range of $10 \le k_1^2 \le 200$ keV. The results show that our values of total H(2s) formation cross sections are in good agreement with those of Choudhury and Sural[21] for incident energy range of $50 \le k_1^2 \le 200$ keV, specially between 150 and 200 keV. The present values of the total H(2s) formation cross sections are larger than those of Choudhury and Sural[21] and smaller than those of Tiwari.[22] The reason for the difference lies in the different approximation used for the scattering wave function and in neglecting the polarization potentials of the target and H(2s) in our calculations. Before leaving this section it is important to mention that further improvements upon the present total collisional cross sections can be also obtained by taking the polarization effect of the hydrogen formation atom in our calculations. We can also consider a three-channel problem by opening H(2p) formation channel.

Table 1. Present partial and total elastic cross sections (σ_{11} in πa_0^2) of p–Na scattering. Integration range is equal to $32a_0$, and the number of iterations $\upsilon = 50$.

k^2/keV	$\ell=0$	$\ell=1$	$\ell=2$	$\ell=3$	$\ell=4$	$\ell=5$	$\ell=6$	σ_{12}
10	3.5672×10^{-2}	9.5125×10^{-3}	1.9025×10^{-3}	3.8050×10^{-4}	7.6100×10^{-5}	1.5220×10^{-5}	3.0440×10^{-6}	4.7562×10^{-2}
20	2.7869×10^{-2}	7.4317×10^{-3}	1.4863×10^{-3}	2.9727×10^{-4}	5.9454×10^{-5}	1.1891×10^{-5}	2.3781×10^{-6}	3.7158×10^{-2}
30	2.1772×10^{-2}	5.8059×10^{-3}	1.1612×10^{-3}	2.3224×10^{-4}	4.6447×10^{-5}	9.2894×10^{-6}	1.8579×10^{-6}	2.9029×10^{-2}
40	1.7010×10^{-2}	4.5359×10^{-3}	9.0718×10^{-4}	1.8144×10^{-4}	3.6287×10^{-5}	7.2574×10^{-6}	1.4515×10^{-6}	2.2679×10^{-2}
50	1.3289×10^{-2}	3.5436×10^{-3}	7.0873×10^{-4}	1.4175×10^{-4}	2.8349×10^{-5}	5.6698×10^{-6}	1.1340×10^{-6}	1.7718×10^{-2}
60	9.5680×10^{-3}	2.5515×10^{-3}	5.1029×10^{-4}	1.0206×10^{-4}	2.0412×10^{-5}	4.0823×10^{-6}	8.1647×10^{-7}	1.2757×10^{-2}
70	6.8891×10^{-3}	1.8371×10^{-3}	3.6742×10^{-4}	7.3484×10^{-5}	1.4697×10^{-5}	2.9393×10^{-6}	5.8787×10^{-7}	9.1853×10^{-3}
80	4.9600×10^{-3}	1.3227×10^{-3}	2.6453×10^{-4}	5.2907×10^{-5}	1.0581×10^{-5}	2.1163×10^{-6}	4.2325×10^{-7}	6.6132×10^{-3}
90	3.5712×10^{-3}	9.5233×10^{-4}	1.9047×10^{-4}	3.8093×10^{-5}	7.6187×10^{-6}	1.5237×10^{-6}	3.0475×10^{-7}	4.7616×10^{-3}
100	2.5713×10^{-3}	6.8568×10^{-4}	1.3714×10^{-4}	2.7427×10^{-5}	5.4854×10^{-6}	1.0971×10^{-6}	2.1942×10^{-7}	3.4283×10^{-3}
110	1.8513×10^{-3}	4.9369×10^{-4}	9.8738×10^{-5}	1.9748×10^{-5}	3.9495×10^{-6}	7.8990×10^{-7}	1.5798×10^{-7}	2.4684×10^{-3}
120	1.3330×10^{-3}	3.5546×10^{-4}	7.1091×10^{-5}	1.4218×10^{-5}	2.8436×10^{-6}	5.6873×10^{-7}	1.1375×10^{-7}	1.7772×10^{-3}
130	9.5970×10^{-4}	2.5592×10^{-4}	5.1184×10^{-5}	1.0237×10^{-5}	2.0474×10^{-6}	4.0947×10^{-7}	8.1895×10^{-8}	1.2796×10^{-3}
140	6.9100×10^{-4}	1.8427×10^{-4}	3.6854×10^{-5}	7.3707×10^{-6}	1.4741×10^{-6}	2.9483×10^{-7}	5.8966×10^{-8}	9.2133×10^{-4}
150	4.9752×10^{-4}	1.3267×10^{-4}	2.6534×10^{-5}	5.3069×10^{-6}	1.0614×10^{-6}	2.1228×10^{-7}	4.2455×10^{-8}	6.6335×10^{-4}
160	3.5821×10^{-4}	9.5524×10^{-5}	1.9105×10^{-5}	3.8209×10^{-6}	7.6419×10^{-7}	1.5284×10^{-7}	3.0568×10^{-8}	4.7761×10^{-4}
170	2.5791×10^{-4}	6.8777×10^{-5}	1.3755×10^{-5}	2.7511×10^{-6}	5.5022×10^{-7}	1.1004×10^{-7}	2.2009×10^{-8}	3.4388×10^{-4}
180	1.8570×10^{-4}	4.9519×10^{-5}	9.9038×10^{-6}	1.9808×10^{-6}	3.9615×10^{-7}	7.9231×10^{-8}	1.5846×10^{-8}	2.4759×10^{-4}
190	1.3370×10^{-4}	3.5654×10^{-5}	7.1308×10^{-6}	1.4262×10^{-6}	2.8523×10^{-7}	5.7046×10^{-8}	1.1409×10^{-8}	1.7827×10^{-4}
200	9.6266×10^{-5}	2.5671×10^{-5}	5.1342×10^{-6}	1.0268×10^{-6}	2.0537×10^{-7}	4.1073×10^{-8}	8.2147×10^{-9}	1.2835×10^{-4}
210	6.9311×10^{-5}	1.8483×10^{-5}	3.6966×10^{-6}	7.3931×10^{-7}	1.4786×10^{-7}	2.9572×10^{-8}	5.9145×10^{-9}	9.2413×10^{-5}
220	4.9905×10^{-5}	1.3308×10^{-5}	2.6616×10^{-6}	5.3232×10^{-7}	1.0646×10^{-7}	2.1293×10^{-8}	4.2585×10^{-9}	6.6539×10^{-5}
230	3.5931×10^{-5}	9.5816×10^{-6}	1.9163×10^{-6}	3.8327×10^{-7}	7.6653×10^{-8}	1.5331×10^{-8}	3.0661×10^{-9}	4.7907×10^{-5}
240	2.5870×10^{-5}	6.8988×10^{-6}	1.3798×10^{-6}	2.7595×10^{-7}	5.5190×10^{-8}	1.1038×10^{-8}	2.2076×10^{-9}	3.4493×10^{-5}
250	1.8626×10^{-5}	4.9671×10^{-6}	9.9341×10^{-7}	1.9868×10^{-7}	3.9737×10^{-8}	7.9473×10^{-9}	1.5895×10^{-9}	2.4835×10^{-5}
300	1.0245×10^{-5}	2.7319×10^{-6}	5.4638×10^{-7}	1.0928×10^{-7}	2.1855×10^{-8}	4.3710×10^{-9}	8.7421×10^{-10}	1.3659×10^{-5}
500	7.1715×10^{-6}	1.9124×10^{-6}	3.8248×10^{-7}	7.6496×10^{-8}	1.5299×10^{-8}	3.0598×10^{-9}	6.1197×10^{-10}	9.5618×10^{-6}
800	5.0199×10^{-6}	1.3386×10^{-6}	2.6773×10^{-7}	5.3546×10^{-8}	1.0709×10^{-8}	2.1418×10^{-9}	4.2837×10^{-10}	6.6931×10^{-6}
1000	3.5139×10^{-6}	9.3705×10^{-7}	1.8741×10^{-7}	3.7482×10^{-8}	7.4964×10^{-9}	1.4993×10^{-9}	2.9986×10^{-10}	4.6852×10^{-6}

Table 2. Present partial and total H(2s) formation cross sections (σ_{12} in πa_0^2) of p–Na scattering. Integration range is equal to $32a_0$, and the number of iterations $\upsilon = 50$.

k^2/keV	$\ell=0$	$\ell=1$	$\ell=2$	$\ell=3$	$\ell=4$	$\ell=5$	$\ell=6$	σ_{12}
10	3.7434×10^{-3}	9.9823×10^{-4}	1.9965×10^{-4}	3.9929×10^{-5}	7.9858×10^{-6}	1.5972×10^{-6}	3.1943×10^{-7}	4.9911×10^{-3}
20	2.9245×10^{-3}	7.7987×10^{-4}	1.5597×10^{-4}	3.1195×10^{-5}	6.2390×10^{-6}	1.2478×10^{-6}	2.4956×10^{-7}	3.8993×10^{-3}
30	2.2847×10^{-3}	6.0926×10^{-4}	1.2185×10^{-4}	2.4371×10^{-5}	4.8741×10^{-6}	9.7482×10^{-7}	1.9496×10^{-7}	3.0463×10^{-3}
40	1.7849×10^{-3}	4.7599×10^{-4}	9.5197×10^{-5}	1.9039×10^{-5}	3.8079×10^{-6}	7.6158×10^{-7}	1.5232×10^{-7}	2.3799×10^{-3}
50	1.3945×10^{-3}	3.7187×10^{-4}	7.4375×10^{-5}	1.4875×10^{-5}	2.9750×10^{-6}	5.9500×10^{-7}	1.1900×10^{-7}	1.8593×10^{-3}
60	1.0041×10^{-3}	2.6775×10^{-4}	5.3550×10^{-5}	1.0710×10^{-5}	2.1420×10^{-6}	4.2840×10^{-7}	8.5680×10^{-8}	1.3387×10^{-3}
70	7.2290×10^{-4}	1.9277×10^{-4}	3.8554×10^{-5}	7.7109×10^{-6}	1.5422×10^{-6}	3.0844×10^{-7}	6.1687×10^{-8}	9.6385×10^{-4}
80	5.2050×10^{-4}	1.3880×10^{-4}	2.7760×10^{-5}	5.5520×10^{-6}	1.1104×10^{-6}	2.2208×10^{-7}	4.4416×10^{-8}	6.9399×10^{-4}
90	3.7476×10^{-4}	9.9936×10^{-5}	1.9987×10^{-5}	3.9974×10^{-6}	7.9948×10^{-7}	1.5990×10^{-7}	3.1979×10^{-8}	4.9967×10^{-4}
100	2.6983×10^{-4}	7.1953×10^{-5}	1.4391×10^{-5}	2.8781×10^{-6}	5.7563×10^{-7}	1.1513×10^{-7}	2.3025×10^{-8}	3.5976×10^{-4}
110	1.9427×10^{-4}	5.1806×10^{-5}	1.0361×10^{-5}	2.0723×10^{-6}	4.1445×10^{-7}	8.2890×10^{-8}	1.6578×10^{-8}	2.5903×10^{-4}
120	1.3988×10^{-4}	3.7301×10^{-5}	7.4602×10^{-6}	1.4920×10^{-6}	2.9841×10^{-7}	5.9682×10^{-8}	1.1936×10^{-8}	1.8650×10^{-4}
130	1.0071×10^{-4}	2.6857×10^{-5}	5.3713×10^{-6}	1.0743×10^{-6}	2.1485×10^{-7}	4.2970×10^{-8}	8.5941×10^{-9}	1.3428×10^{-4}
140	7.2512×10^{-5}	1.9337×10^{-5}	3.8673×10^{-6}	7.7346×10^{-7}	1.5469×10^{-7}	3.0938×10^{-8}	6.1877×10^{-9}	9.6681×10^{-5}
150	5.2209×10^{-5}	1.3922×10^{-5}	2.7845×10^{-6}	5.5690×10^{-7}	1.1138×10^{-7}	2.2276×10^{-8}	4.4552×10^{-9}	6.9611×10^{-5}
160	3.7590×10^{-5}	1.0024×10^{-5}	2.0048×10^{-6}	4.0096×10^{-7}	8.0193×10^{-8}	1.6039×10^{-8}	3.2077×10^{-9}	5.0120×10^{-5}
170	2.7065×10^{-5}	7.2174×10^{-6}	1.4435×10^{-6}	2.8870×10^{-7}	5.7739×10^{-8}	1.1548×10^{-8}	2.3096×10^{-9}	3.6086×10^{-5}
180	1.9487×10^{-5}	5.1965×10^{-6}	1.0393×10^{-6}	2.0786×10^{-7}	4.1572×10^{-8}	8.3144×10^{-9}	1.6629×10^{-9}	2.5982×10^{-5}
190	1.4031×10^{-5}	3.7415×10^{-6}	7.4830×10^{-7}	1.4966×10^{-7}	2.9932×10^{-8}	5.9864×10^{-9}	1.1973×10^{-9}	1.8707×10^{-5}
200	1.1632×10^{-5}	3.1018×10^{-6}	6.2037×10^{-7}	1.2407×10^{-7}	2.4815×10^{-8}	4.9629×10^{-9}	9.9259×10^{-10}	1.5509×10^{-5}
210	7.2734×10^{-6}	1.9396×10^{-6}	3.8792×10^{-7}	7.7583×10^{-8}	1.5517×10^{-8}	3.1033×10^{-9}	6.2067×10^{-10}	9.6977×10^{-6}
220	5.2369×10^{-6}	1.3965×10^{-6}	2.7930×10^{-7}	5.5860×10^{-8}	1.1172×10^{-8}	2.2344×10^{-9}	4.4688×10^{-10}	6.9824×10^{-6}
230	3.7705×10^{-6}	1.0055×10^{-6}	2.0110×10^{-7}	4.0219×10^{-8}	8.0438×10^{-9}	1.6088×10^{-9}	3.2175×10^{-10}	5.0273×10^{-6}
240	2.7148×10^{-6}	7.2395×10^{-7}	1.4479×10^{-7}	2.8958×10^{-8}	5.7916×10^{-9}	1.1583×10^{-9}	2.3166×10^{-10}	3.6197×10^{-6}
250	1.9547×10^{-6}	5.2125×10^{-7}	1.0425×10^{-7}	2.0850×10^{-8}	4.1700×10^{-9}	8.3400×10^{-10}	1.6680×10^{-10}	2.6062×10^{-6}
300	1.3436×10^{-6}	3.5828×10^{-7}	7.1656×10^{-8}	1.4331×10^{-8}	2.8663×10^{-9}	5.7325×10^{-10}	1.1465×10^{-10}	1.7914×10^{-6}
500	3.6069×10^{-7}	9.6183×10^{-8}	1.9237×10^{-8}	3.8473×10^{-9}	7.6947×10^{-10}	1.5389×10^{-10}	3.0779×10^{-11}	4.8091×10^{-7}
800	1.9164×10^{-7}	5.1104×10^{-8}	1.0221×10^{-8}	2.0442×10^{-9}	4.0883×10^{-10}	8.1766×10^{-11}	1.6353×10^{-11}	2.5552×10^{-7}
1000	1.7992×10^{-8}	4.7978×10^{-9}	9.5955×10^{-10}	1.9191×10^{-10}	3.8382×10^{-11}	7.6764×10^{-12}	1.5353×10^{-12}	2.3988×10^{-8}

Table 3. Present total H(2s) cross-section formation (σ_{12} in πa_0^2) of p–Na scattering together with theoretical results (Refs. [21] and [22]).

k^2/keV	σ_{12}		
	Present	Ref. [21]	Ref. [22]
50	1.8593×10^{-3}	1.16×10^{-3}	5.269×10^{-3}
60	1.3387×10^{-3}	–	–
70	9.6385×10^{-4}	–	–
80	6.9399×10^{-4}	–	–
100	3.5976×10^{-4}	8.27×10^{-5}	4.912×10^{-3}
150	6.9612×10^{-5}	2.41×10^{-5}	1.827×10^{-3}
200	1.5509×10^{-5}	1.03×10^{-5}	5.206×10^{-4}
250	2.6062×10^{-6}	–	–
500	4.8092×10^{-7}	2.91×10^{-7}	6.022×10^{-7}
800	2.5552×10^{-7}	–	1.029×10^{-7}
1000	2.3989×10^{-8}	–	1.105×10^{-8}

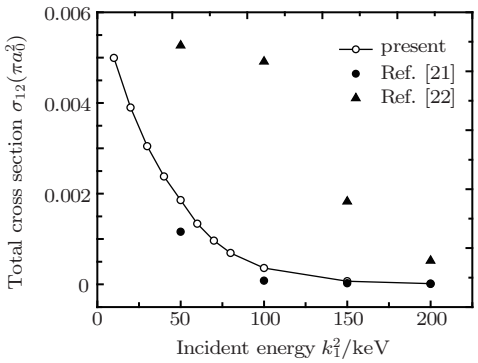


Fig. 2. Present total H(2s) formation cross sections (σ_{12} in πa_0^2) of p–Na scattering together with theoretical results (Refs. [21] and [22]).

4. Conclusions

It is interesting to mention that all theoretical techniques applied to the collisions of electron with atoms can be extended to proton–atom collisions after allowing for hydrogen formation channel instead of recombination channel. Proton–sodium inelastic scattering is studied using the coupled static approximation. Our interest is focused on the influence of producing H(2s) atom in the second channel. The present calculations of the total H(2s) formation cross sections using the coupled static approximation show a reasonable agreement with available theoretical calculations in a wide region of incident energies.

Acknowledgments

The author would like to express his deep gratitude to Prof. M. A. Abdel-Raouf for his interest in this work and useful discussion.

Appendix A

Our main goal in this appendix is to calculate the reactance matrix $\boldsymbol{R}$.

Let us consider the partial wave expansions of the scatter-

ing wave functions $|\psi_1\rangle$ and $|\psi_2\rangle$, i.e.,

$$\psi_1 = \frac{1}{x}\sum(2\ell+1)\mathrm{i}^\ell f_\ell(x)\mathrm{Y}^0_\ell(\hat{x}), \tag{A1}$$

$$\psi_2 = \frac{1}{\sigma}\sum(2\ell+1)\mathrm{i}^\ell g_\ell(\sigma)\mathrm{Y}^0_\ell(\hat{\sigma}), \tag{A2}$$

where $f_\ell(x)$ and $g_\ell(x)$ are the radial partial wave functions corresponding to the total angular momentum ℓ of the first and second channels, respectively, $\mathrm{Y}^0_\ell(\hat{x})$ and $\mathrm{Y}^0_\ell(\hat{\sigma})$ are the related spherical harmonics, $\hat{x}$ and $\hat{\sigma}$ are the angles between the vectors $\bar{x}$ and $\bar{\sigma}$ and the z axis.

Substituting Eqs. (A1) and (A2) into Eqs. (23) and (24), we obtain for each value of ℓ, the following coupled integro-differential equations

$$\left[\frac{\mathrm{d}^2}{\mathrm{d}x^2} - \frac{\ell(\ell+1)}{x^2} + k_1^2\right] f_\ell(x) = 2\mu_\mathrm{M} U^{(1)}_\mathrm{st}(x) f_\ell(x) + \int_0^\infty K_{12}(x,\sigma) g_\ell(\sigma)\,\mathrm{d}\sigma, \tag{A3}$$

$$\left[\frac{\mathrm{d}^2}{\mathrm{d}\sigma^2} - \frac{l(l+1)}{\sigma^2} + k_2^2\right] g_\ell(\sigma) = 2\mu_{\mathrm{M}'} U^{(2)}_\mathrm{st}(\sigma) g_\ell(\sigma) + \int_0^\infty K_{21}(x,\sigma) f_\ell(x)\,\mathrm{d}x, \tag{A4}$$

where the Kernels K_{12} and K_{21} are expanded by

$$K_{12}(x,\sigma) = 2\mu_\mathrm{M}(8\sigma x)\iint \Phi_{\mathrm{Na(3s)}}(r)\,\Phi_{\mathrm{H(2s)}}(\rho) \times\left[-\frac{1}{2\mu_{\mathrm{M}'}}\left(\nabla^2_\sigma + k_2^2\right) + V^{(2)}_\mathrm{int}\right] \times \mathrm{Y}^o_\ell(\hat{x})\,\mathrm{Y}^o_\ell(\hat{\sigma})\,\mathrm{d}\hat{x}\mathrm{d}\hat{\sigma}, \tag{A5}$$

$$K_{21}(x,\sigma) = 2\mu_{\mathrm{M}'}(8\sigma x)\iint \Phi_{\mathrm{Na(3s)}}(r)\,\Phi_{\mathrm{H(2s)}}(\rho) \times\left[-\frac{1}{2\mu_\mathrm{M}}\left(\nabla^2_x + k_1^2\right) + V^{(1)}_\mathrm{int}\right] \mathrm{Y}^o_\ell(\hat{x}) \times \mathrm{Y}^o_\ell(\hat{\sigma})\,\mathrm{d}\hat{x}\mathrm{d}\hat{\sigma}. \tag{A6}$$

The number 8 appearing in the preceding equations refers to the Jacobian of the transformations $\int \mathrm{d}r \to 8\int \mathrm{d}\sigma$ and $\int \mathrm{d}\rho \to 8\int \mathrm{d}x$.

Let us now rewrite Eqs. (A3) and (A4) as

$$\left[\frac{\mathrm{d}^2}{\mathrm{d}x^2} - \frac{\ell(\ell+1)}{x^2} + k_1^2\right] f_\ell(x) = 2\mu_\mathrm{M} U^{(1)}_\mathrm{st}(x) f_\ell(x) + Q_1(x), \tag{A7}$$

$$\left[\frac{\mathrm{d}^2}{\mathrm{d}\sigma^2} - \frac{\ell(\ell+1)}{\sigma^2} + k_2^2\right] g_\ell(x) = 2\mu_{\mathrm{M}'} U^{(2)}_\mathrm{st}(\sigma) g_\ell(\sigma) + Q_2(\sigma), \tag{A8}$$

where

$$Q_1(x) = \int_0^\infty K_{12}(x,\sigma) g_\ell(\sigma)\,\mathrm{d}\sigma, \tag{A9}$$

$$Q_2(\sigma) = \int_0^\infty K_{21}(x,\sigma) f_\ell(x)\,\mathrm{d}x. \tag{A10}$$

The solutions of Eqs. (A7) and (A8) are given formally (using Lippmann–Schwinger equation) by

$$f^{(i)}_\ell(x) = \left\{\delta_{i1} + \frac{1}{k_1}\int_0^\infty \tilde{g}_\ell(k_1x')\left[2\mu_\mathrm{M}U^{(1)}_\mathrm{st}(x') f^{(i)}_\ell(x') + Q^{(i)}_1(x')\right]\mathrm{d}x'\right\}_1 \tilde{f}_\ell(k_1x) + \left\{-\frac{1}{k_1}\int_0^\infty \tilde{f}_\ell(k_1x')\left[2\mu_\mathrm{M}U^{(1)}_\mathrm{st}(x') f^{(i)}_\ell(x') + Q^{(i)}_1(x')\right]\mathrm{d}x'\right\}_2 \tilde{g}_\ell(k_1x), \quad i=1,2, \tag{A11}$$

$$g^{(i)}_\ell(\sigma) = \left\{\delta_{i2} + \frac{1}{k_2}\int_0^\infty \tilde{g}_\ell(k_2\sigma')\left[2\mu_{\mathrm{M}'}U^{(2)}_\mathrm{st}(\sigma') g^{(i)}_\ell(\sigma') + Q^{(i)}_2(\sigma')\right]\mathrm{d}\sigma'\right\}_3 \tilde{f}_\ell(k_2\sigma) + \left\{-\frac{1}{k_2}\int_0^\infty \tilde{f}_\ell(k_2\sigma')\left[2\mu_{\mathrm{M}'}U^{(2)}_\mathrm{st}(\sigma') g^{(i)}_\ell(\sigma') + Q^{(i)}_2(\sigma')\right]\mathrm{d}\sigma'\right\}_4 \tilde{g}_\ell(k_2\sigma), \quad i=1,2, \tag{A12}$$

where the delta functions δ_{ij} $(i,j=1,2)$ specify two independent forms of solutions for each $f_\ell(x)$ and $g_\ell(\sigma)$ in channels $i=1,2$, according to the channel considered. Thus, if $i=1$, the first element in the bracket of $\tilde{f}_\ell(x)$, for example, will be 1, defining the first form of solution. For $i=2$ this element will be zero, defining the second form. The functions $\tilde{f}_\ell(\mu)$ and $\tilde{g}_\ell(\mu)$, $\mu = k_1x$ or $k_2\sigma$, are related to the Bessel functions of the first and second channels, i.e., $j_\ell(m)$ and $y_\ell(m)$, respectively, by the relations $\tilde{f}_\ell(\mu) = \mu j_\ell(\mu)$ and $\tilde{g}_\ell(\mu) = -my_\ell(\mu)$. It is obvious from Eqs. (A11) and (A12) that the solutions can be only found iteratively and the v-th iteration is calculated by

$$f^{(i,v)}_\ell(x) = \left\{\delta_{i1} + \frac{1}{k_1}\int_0^X \tilde{g}_\ell(k_1x')\left[2\mu_\mathrm{M}U^{(1)}_\mathrm{st}(x') f^{(i,v)}_\ell(x') + Q^{(i,v-1)}_1(x')\right]\mathrm{d}x'\right\}_1 \tilde{f}_\ell(k_1x) + \left\{-\frac{1}{k_1}\int_0^X \tilde{f}_\ell(k_1x')\left[2\mu_\mathrm{M}U^{(1)}_\mathrm{st}(x') f^{(i,v)}_\ell(x') + Q^{(i,v-1)}_1(x')\right]\mathrm{d}x'\right\}_2 \tilde{g}_\ell(k_1x), \quad i=1,2,;v\geq 1, \tag{A13}$$

and

$$g^{(i,v)}_\ell(\sigma) = \left\{\delta_{i2} + \frac{1}{k_1}\int_0^\Sigma \tilde{g}_\ell(k_2\sigma')\left[2\mu_{\mathrm{M}'}U^{(2)}_\mathrm{st}(x') g^{(i,v)}_\ell(\sigma') + Q^{(i,v)}_2(\sigma')\right]\mathrm{d}\sigma'\right\}_3 \tilde{f}_\ell(k_2\sigma) + \left\{-\frac{1}{k_2}\int_0^\Sigma \tilde{f}_\ell(k_2\sigma')\left[2\mu_{\mathrm{M}'}U^{(2)}_\mathrm{st}(\sigma') g^{(i,v)}_\ell(\sigma') + Q^{(i,v)}_2(\sigma')\right]\mathrm{d}\sigma'\right\}_4 \tilde{g}_\ell(k_2\sigma), \quad i=1,2,;v\geq 0, \tag{A14}$$

The zeroth iteration of $f_\ell^{(i,0)}(x)$ is obtained by

$$f_\ell^{(i,0)}(x) = \left\{ \delta_{i1} + \frac{1}{k_1}\int_0^X \tilde{g}_\ell(k_1 x') \times \left[2\mu_M U_{st}^{(1)}(x') f_\ell^{(i,0)}(x')\right] dx' \right\}_1 \tilde{f}_\ell(k_1 x) + \left\{ -\frac{1}{k_1}\int_0^X \tilde{f}_\ell(k_1 x') \times \left[2\mu_M U_{st}^{(1)}(x') f_\ell^{(i,0)}(x')\right] dx' \right\}_2 \tilde{g}_\ell(k_1 x), \quad i = 1,2, \tag{A15}$$

where X and Σ specify the integration range (IR) away from the nucleus over which the integrals Eqs. (A13)–(A15) are calculated using Simpson's expansions. The functions $Q_1^{(i,\nu-1)}(x')$ and $Q_2^{(i,\nu)}(\sigma')$, in Eqs. (A13) and (A14), are now defined by

$$Q_1^{(i,\nu-1)}(x') = \int_0^\Sigma K_{12}(x',\sigma) g_\ell^{(i,\nu-1)}(\sigma') d\sigma', \quad \nu \geq 1, \tag{A16}$$

$$Q_2^{(i,\nu)}(\sigma') = \int_0^X K_{21}(x,\sigma') f_\ell^{(i,\nu)}(x) dx, \quad \nu \geq 0. \tag{A17}$$

Thus, the iteration process starts by calculating $f_\ell^{(i,0)}(x)$, $i = 1,2$, using Eq. (A15) and introducing its values into Eq. (A17) in order to find $Q_2^{(i,0)}(\sigma')$ which can be used in the right-hand side of Eq. (A14) for obtaining $g_\ell^{(i,0)}(\sigma)$. The values of the last quantity can be introduced into Eq. (A16) in order to calculate $Q_1^{(i,0)}(x')$ which may be used in Eq. (A13) for determining $f_\ell^{(i,1)}(x)$. This iteration process can be repeated as many times as we need and the judge of its quantity is the stationary variation of the elements of the reactance matrix R_{ij}^ν where ν increases (note: $f_\ell^{(i,\nu)}(0) = g_\ell^{(i,\nu)}(0) = 0$.) In order to find the starting value of $f_\ell^{(i,0)}(x)$, we consider the Taylor expansion of $U_{st}^{(1)}(x)$, $\tilde{f}_\ell(k_1 x)$, and $\tilde{g}_\ell(k_1 x)$ around the origin. For further information about the numerical techniques employed in this paper, see Ref. [13].

Equations (A13) and (A14) can be abbreviated to

$$f_\ell^{(i,\upsilon)}(x) = a_1^{(i,\upsilon)} \tilde{f}_\ell(k_1 x) + b_1^{(i,\upsilon)} \tilde{g}_\ell(k_1 x), \quad i = 1,2, \tag{A18}$$

$$g_\ell^{(i,\upsilon)}(\sigma) = a_2^{(i,\upsilon)} \tilde{f}_\ell(k_2 \sigma) + b_2^{(i,\upsilon)} \tilde{g}_\ell(k_2 \sigma), \quad i = 1,2, \tag{A19}$$

where

$$a_1^{(i,\upsilon)} = \{\}_1, \quad b_1^{(i,\upsilon)} = \{\}_2,$$

$$a_2^{(i,\upsilon)} = \{\}_3, \quad b_2^{(i,\upsilon)} = \{\}_4.$$

The coefficients in Eqs. (A18) and (A19) are elements of the following matrices:

$$\boldsymbol{a}^\upsilon = \begin{pmatrix} \sqrt{2\mu_M/k_1}\, a_1^{(1,\upsilon)} & \sqrt{2\mu_M/k_1}\, a_1^{(2,\upsilon)} \\ \sqrt{2\mu_{M'}/k_2}\, a_2^{(1,\upsilon)} & \sqrt{2\mu_{M'}/k_2}\, a_2^{(2,\upsilon)} \end{pmatrix},$$

$$\boldsymbol{b}^\upsilon = \begin{pmatrix} \sqrt{2\mu_M/k_1}\, b_1^{(1,\upsilon)} & \sqrt{2\mu_M/k_1}\, b_1^{(2,\upsilon)} \\ \sqrt{2\mu_{M'}/k_2}\, b_2^{(1,\upsilon)} & \sqrt{2\mu_{M'}/k_2}\, b_2^{(2,\upsilon)} \end{pmatrix}, \tag{A20}$$

which are connected with the reactance matrix, $\boldsymbol{R}^\upsilon$, through the relation

$$\boldsymbol{R}^\upsilon = \boldsymbol{b}^\upsilon (\boldsymbol{a}^\upsilon)^{-1}. \tag{A21}$$

References

[1] Abdel-Raouf M A 1988 *J. Phys. B* **21** 2331
[2] Elkilany S A 1995 *IL Nuovo Cimento* **17D** 1
[3] Elkilany S A 1996 *IL Nuovo Cimento* **109A** 1
[4] Elkilany S A 1997 *IL Nuovo Cimento* **19D** 1525
[5] Elkilany S A 1998 *IL Nuovo Cimento* **20D** 147
[6] Surdutovich E, Johnson J M, Kauppila W K, Kwan C K and Stein T S 2002 *Phys. Rev. A* **65** 032713
[7] Jun G N, Jun Z Y and Qi K Y 2004 *Chin. Phys. Lett.* **21** 2406
[8] Roy U and Ho Y K 2004 *Nuclear Instruments and Methods in Physics Research* **B221** 36
[9] Gilmore S, Blackwood J E and Walters H R J 2004 *Nuclear Instruments and Methods in Physics Research* **B221** 124
[10] Ratnavelu K and Ng S Y 2006 *Chin. Phys. Lett.* **23** 1753
[11] Abdel-Raouf M A and Elkilany S A 2009 *J. Phys. B* **194** 072004
[12] Abdel-Raouf M A and Elkilany S A 2009 *Int. J. Pure Appl. Phys.* **5** 93
[13] Elkilany S A 2009 *Int. J. Pure Appl. Phys.* **5** 101
[14] Jun C Y, Jun Z Y and Fang L 2011 *Chin. Phys. Lett.* **28** 123403
[15] Fang L, Jun C Y and Jun Z 2012 *Chin. Phys. B* **21** 053403
[16] Banyard K E and Shirtcliffe G W 1979 *J. Phys. B* **12** 3247
[17] Ferrante G, Fiordilino E and Zarcone M 1979 *IL Nuovo Cimento* **52B** 151
[18] Daniele R, Ferrante G and Fiordilino E 1979 *IL Nuovo Cimento* **54B** 185
[19] Ferrante Gand Fiordilino E 1980 *IL Nuovo Cimento* **57B** 1
[20] Fritsch W and Lin C D 1983 *J. Phys. B* **16** 1595
[21] Choudhury K B and Sural D P 1992 *J. Phys. B* **25** 853
[22] Tiwari Y N 2008 *Pramana-J. Phys.* **70** 753
[23] Elkilany S A and Abdel-Raouf M A 2012 *J. Phys. B* **388** 072030
[24] Elkilany S A 2014 *Indian J. Phys.* **88** 19
[25] Elkilany S A 2014 *J. Theor. Chem.* **2014** 1
[26] Clementi E and Roetti C 1974 *Atomic Data Nuclear Data Tables* **14** 177